Available online at www.sciencedirect.com

ScienceDirect

Procedia Structural Integrity 12 (2018) 507–520

Structural Integrity Procedia

www.elsevier.com/locate/procedia

AIAS 2018 International Conference on Stress Analysis

Modeling the effects of tolerances and assembly errors on the optical performances of parabolic collectors in a concentrating solar power system

F. Cadini[a*], M. Fossati[a], M. Donati[a], S. Cardamone[a], M. Giglio[a]

[a]*Politecnico di Milano, Dipartimento di Meccanica,via La Masa 1, 20156 Milano, Italy*

Abstract

The major problem related to the implementation of Concentrating Solar Power (CSP) systems is related to their Levelized Cost of Electricity (LCOE), which is still higher than that associated to other energy production methods, thus limiting their competitiveness. It is widely recognized that large cost savings can still be achieved by improving the collector and solar field designs. In this context, one important issue is that, currently, very detailed analyses of CSP components' production tolerances and assembly/mounting errors are performed in order to guarantee the desired optical performances of a CSP plant. Unfortunately, these analyses require very large computational efforts, so that full design optimizations, implying many model runs, become almost impractical. Hence, the main objective of this work is that of developing new, lean methodologies, still relying on proper experimental knowledge, for supporting the CSP system optimal design at affordable computational expenses. The methodological approach stems from an extension of a semi-analytic model of literature for the calculation of the intercept factor, i.e., an important optical efficiency parameter. The proposed modifications explicitly account for the effects of the production tolerances and assembly/mounting errors by including simple, parameterized FEM calculations and geometric considerations. After properly casting the problem into a probabilistic framework, we exploit the simplicity and computational speed of the proposed model in order to perform a Sobol-based global sensitivity analysis (GSA) of the CSP optical performances. From a purely engineering point of view, the results of this kind of analysis provide fundamental insights for supporting a decision-making process aimed at optimizing the CSP component production and the solar plant assembly/mounting at a full power production scale.

Keywords: Solar energy; parabolic trough collector; optical efficiency; sensitivity analysis; optimization, cost minimization, genetic algorithms.

1. Introduction

The Concentrating Solar Power (CSP) technology is a modern power generation strategy based on the use of properly designed mirrors capable of concentrating the sun's rays on a focal point (or line), thus increasing the temperature of a thermo-vector fluid. In most of today's CSP systems, this heat is used to produce steam, which is then used to drive conventional steam turbines cycle.

Despite the sunrays properties have been known since the ancient time, the adoption of this technique for the energy production on a large scale is rather recent, more recent than photovoltaic (PV) technology, which is nowadays rather spread out,

* Corresponding author. Tel.: +39-02-2399-6355.
E-mail address: francesco.cadini@polimi.it

10.1016/j.prostr.2018.11.067

with a total installed capacity at the end of 2016 of 303 gigawatts (GW). On the other hand, the CSP technology total installed capacity remained quite low until not too much time ago: at the end of 2005, in fact, it was approximately equal to 354 MW. Since then it has rapidly grown, and, at the end of 2016, it reached approximately 5 GW, still much lower, however, than that obtained by PV power plants. Furthermore, from 2009, annual CSP investments have increased by nearly 280% to $6.9 billion, as reported by Mehos et al. (2016).

Many studies, such as those of Fend and Qoaider (2011) or Dinter and Gonzalez (2013), confirm that the main characteristic of CSP systems, which has drawn the attention of many investors and countries, is the possibility to accumulate energy by Thermal Energy Storage (TES) systems and use it during the night. This allows for generating electricity for base load exactly like traditional thermal power plants, despite the fact that the solar irradiation is not available 24 h/day.

The major problem related to the implementation of this technology is related to their Levelized Cost of Electricity (LCOE), which is still higher than those associated to other energy production methods, thus limiting their competitiveness, as reported by IRENA (2015). However, in the last few years, governments are trying to make strong efforts, in the form of tax breaks, granting of debts, and so on, in order to support solar power generation technologies and, at the same time, accelerate its deployment, bringing technology improvements and cost reductions. For example, the SunShot initiative, promoted by the U.S Department of Energy, helps and improves the growth of the CSP technology with the aim of reducing the associated LCOE from 0.21 USD/Kwh in 2010 to 0.06 USD/Kwh by 2020, according to the U.S. Department of Energy (2017). A large part of the cost reduction is related to the technological improvement of the collectors' design and of the solar field as a whole, since they are responsible for almost 40% of the LCOE.

In this general context, the main objective of this work is that of developing new computational tools and using the proper experimental knowledge (gained at the Politecnico di Milano during the construction of a CSP prototype in collaboration with ENI) in order to be able to provide guidance in the definition of the CSP components' production tolerances (dimensional and/or geometric) and assembly/mounting errors which should guarantee the desired optical performances of a CSP solar power plant, without taking into account the effects of external agents affecting the collectors' structures (e.g., winds, dust accumulation, gravity, etc). In other words, the methodological approach proposed in this work, properly supported by experimental knowledge, aims at becoming an effective support in the definition of the quality control procedures necessary both in the design of solar collectors and implementation phases.

In order to achieve this goal, we initially extend a semi-analytic model developed by Bendt et al. (1979) for the calculation of the intercept factor (which significantly affects the optical efficiency of this kind of solar collectors) in order to be able to account for the effects of the CSP components' production tolerances and assembly/mounting errors. Typically, in fact, the semi-analytical models used to evaluate the optical efficiency of a solar collector identify a few general sources of errors (such as those due to imperfections of the reflective surfaces, tracking, displacements of the receiver or the collectors, etc.), but do not delve into the root causes of these errors (or, alternatively, deviations from the ideal, perfect behavior), which, in the end, are to be always sought after the component's tolerances and their assembly/mounting errors. Moreover, often probability distributions are used to account for their effects, thus losing any local, more detailed information. On the other hand, detailed numerical models, such as combinations of FEM and ray-tracing numerical codes, can also be used, but, due to the complexity of the resulting models and to their specificity with respect to the structure under analysis, they can hardly be used for sensitivity analysis or optimization purposes. In this work, we originally propose to overcome these problems by explicitly modelling the effects of the most important tolerances and errors on the deviations of the reflected solar rays from their ideal (design) trajectories within the classical, semi-analytical framework taken from Bendt et al. (1979). The proposed models rely on both very simple FEM calculations and geometric considerations. The most important tolerances and errors included in the modelling framework are here identified by means of a procedure based on the engineering common sense for pre-screening a quite complete list of components and assembly/mounting phases (derived from the experience gained during the construction of the CSP prototype at the Politecnico di Milano) potentially contributing to the total optical error.

The resulting model turns out to be simple and fast enough to allow the calculation of the intercept factor in correspondence of different sets of tolerance/error values at negligible computational times. Thus, complex analyses requiring many repeated calculations become computationally affordable, such as those typically required in problems involving a probabilistic treatment of the various uncertainties involved (i.e., for example, the tolerances and the errors of our context).

More specifically, after properly casting the problem under analysis into a probabilistic framework, we first exploit the proposed modelling framework in order to innovatively perform a sensitivity analysis (SA) of the CSP optical performances with respect to the pre-selected production tolerances and assembly/mounting errors. From a purely engineering point of view, the results of this kind of analysis provide fundamental insights for supporting a decision-making process aimed at optimizing the CSP component production and the solar plant assembly/mounting at an actual power production scale. Furthermore, in this work we propose to resort to two different SA strategies: we start with a fast, but very rough, local approach, namely the "nominal range sensitivity analysis" and we then refine the results by applying a more complete, global algorithm based on the estimation of the Sobol indices derived from the ANOVA decomposition.

The paper is organized as follows. Section 2 initially recalls the basis of the semi analytical model of literature for the calculation of the intercept factor Bendt et al. (1979); then, in Section 3, the modifications are introduced in the model to account for manufacturing tolerances and assembly/mounting errors are illustrated. Section 4 briefly introduces the sensitivity analysis techniques adopted in this work, focusing in particular on the global approach based on the estimation of the Sobol indexes. The complete model for the calculation of the intercept factor is then used to obtain the results both of a simple local sensitivity

analysis based on the nominal range sensitivity analysis, and the more complete and complex global sensitivity analysis for the identification of the tolerances/errors most influencing the CSP intercept factor. Some conclusions are drawn in Section 5.

2. Semi-analytical model for the intercept factor calculation

2.1. Semi analytical model for the calculation of the intercept factor of a parabolic trough

This Section briefly reviews the basics of the approach proposed by Bendt et al. (1979). The interested reader is referred to Bendt et al. (1979) for a thorough description of the model and for the exemplifying figures and tables. The reasons behind the choice of this kind of semi-analytical model are related to the fact that "ray-tracing" methods, typically used to calculate the optical efficiencies of solar systems, provide very detailed information from the point of view of the final result (intercept factor, optical efficiency), but "obscure" the existing relationships between the input parameters and the efficiency. However, functional relationships are indeed critical to the development of design and optimization procedures for engineering system in general, and thus in particular for parabolic trough-based CSP systems.

The first fundamental assumption of the original model is that of reducing the complete three-dimensional problem into a bi-dimensional one, thus significantly simplifying the mathematical approach. The simplification, which stems from a fundamental property of parabolic trough collectors, amounts to restricting the analysis only to the projections of the incident and reflected solar rays on the transversal *xy* plane of the trough. In fact, for a given incident angle $\theta_{i,xy}$ in the *xy* plane, regardless the rays inclination with respect to the parabolic trough longitudinal axis *z*, the *xy* projections of the reflected rays are always the same (i.e, the reflection angle $\theta_{r,xy}$ does not change). This simplification indeed introduces some errors, mainly related to the losses at the trough edges, but in most operating conditions they can be considered negligible, according to Bendt et al. (1979).

Then, it is assumed that any errors affecting the optical efficiency can be modeled as rotations of the reflecting surface (and not as rigid displacements), which generate deviations $\Delta\theta$ (typically expressed in [mrad]) of the normal $\vec{\boldsymbol{n}}$ to the surface at the point of reflection, with respect of the nominal (or ideal) design direction. The error is described by means of two angular variables, called $d\omega_{\parallel}$ and $d\omega_{\perp}$, which refer to the rotations of $\vec{\boldsymbol{n}}$ in the parallel and perpendicular plane, respectively, with respect to the trough longitudinal *z* axis.

Considering now the error distributions $d\omega_{\parallel}$ and $d\omega_{\perp}$, supposing that they are independent and described by distributions with standard deviations respectively $\sigma_{\parallel}$ and $\sigma_{\perp}$, Bendt et al. (1979) showed that the consequent distribution of the projected angles depends on both effects and it is described by a distribution with a total variance $\sigma^2_{contour}$ given by Eq. 1.

$$\sigma^2_{contour} = 4\sigma^2_{\perp} + 4n^2_x \cdot tan^2\theta_{\parallel} \cdot \sigma^2_{\parallel} \tag{1}$$

These errors associated to the macroscopic rotations of the reflecting surface, due to deviations from the ideal parabolic profile of the trough caused by constructive tolerances and assembly errors, and they are thus generally labeled as contour errors.

This last equation depends on the time of the day (through $\theta_{\parallel}$) and on the incidence point of solar radiation (through n^2_x). Note that ray-tracing approaches strictly refer to Eq. 1, whereas, in the present semi-analytical model, it is more convenient to replace this equation with another one where the above varying parameters are averaged on the arc of the day and on the whole opening of the parabola. This approximation is reinforced by the fact that the errors introduced are in general rather small, due to the small value assumed by the parameters $\theta_{\parallel}$ and n^2_x in real applications.

The equation resulting from this averaging operation, including the aforementioned simplifications, becomes:

$$\sigma^2_{contour} = 4\sigma^2_{\perp} + 4\langle n^2_x\rangle \cdot \langle tan^2\theta_{\parallel}\rangle \cdot \sigma^2_{\parallel} \tag{2}$$

where $\langle n^2_x\rangle$ represents the average n^2_x on the entire parabola's opening, whereas $\langle tan^2\theta_{\parallel}\rangle$ represents the average $tan^2\theta_{\parallel}$ on the entire day.

Table 2-1 in Bendt et al. (1979), not reported here for brevity's sake, shows an example of these values obtained for parabolic concentrators with east-west rotation axis, expressed as a function of the aperture's angle of the parabola (called *rim angle* Φ) and the cut-off time, that means the hours after the sunrise and before sunset which define the useful time range of parabolic operation. In general, for parabola tracer with North-South axis, the second term of Eq. 2 becomes very small compared to the first term and can therefore be neglected.

In addition to the errors above, associated to the *macroscopic* rotations of the reflecting surface, other types of errors should generally be included in the analysis. Among them, we recall the loss of perfect specularity of the reflective material (with contribution both on parallel and on perpendicular component, similar to the contour errors) that can be considered due to *microscopic* rotations of the reflecting surface, incorrect mirror-receiver positioning and incorrect tracking. All these phenomena give rise to a further dispersion of the reflected rays, thus globally reducing the optical efficiency. Expressing the variance of the distributions of these errors respectively as $\sigma^2_{specular}$, $\sigma^2_{displacement}$ and $\sigma^2_{tracking}$, Eq. 2 can be integrated and rewritten as:

$$\sigma^2_{optical} = 4\sigma^2_{contour,\perp} + \sigma^2_{specular,\perp} + \lambda(\Phi)\cdot\left(4\sigma^2_{contour,\parallel} + \sigma^2_{specular,\parallel}\right) + \sigma^2_{displacement} + \sigma^2_{tracking} \tag{3}$$

where the function $\lambda(\Phi)$ of the rim angle Φ is defined as:

$$\lambda(\Phi) = \langle n_x^2 \rangle \cdot \langle tan^2 \theta_{\parallel} \rangle \tag{4}$$

The total optical errors' variance, $\sigma^2_{optical}$, can be obtained through Eq. 3 independently of the type of distribution of the errors considered (the various contributions do not necessarily have to be all distributed according to a Gaussian probability density function-pdf), since, in case they are independent, the central limit theorem guarantees that the optical error distribution, which, being the total reflected angle deviation, is the sum of the various errors mentioned above, tends to be distributed according to a Gaussian pdf, whose variance is given by the sum of the variances of the distributions of the individual errors.

Rigorously, the errors $\sigma^2_{displacement}$ and $\sigma^2_{tracking}$ should be single valued, thus not described by probability distributions. However, their distribution should be considered when the analysis is extended to a sufficiently large field of parabolic collectors (both for $\sigma^2_{displacement}$ and $\sigma^2_{tracking}$) and when considering their operation in a sufficient long working time (only for $\sigma^2_{tracking}$). In the present work, for simplicity, but with no loss of generality, we will not consider the contribution of the tracking and specular errors (represented by $\sigma^2_{tracking}$ and $\sigma^2_{specular}$) and we will propose a modeling of the effect of tolerances and assembly errors on optical efficiency through contour and displacement errors (represented by $\sigma^2_{contour}$ and $\sigma^2_{displacement}$).

2.2. Calculation of the effective source distribution

As we as seen in the previous Section, when a sunray hits a reflecting surface, it is reflected in a certain direction, according to the reflection's laws, and if this surface deviates with respect to the ideal profile, a further deviation of the reflected ray is induced compared to the ideal project design. By relying on the optical laws, we can link the deviations suffered by the reflected ray to the errors which, as shown above, are expressed as rotations of the reflecting surface elements. Denoting with θ_{slope} the angle representing the rotation of the reflecting surface in the *xy* plane with respect to the ideal surface, the resulting deviation of the reflected ray θ_{proj} from the ideal, or design, direction can be obtained by multiplying by two θ_{slope}, yielding:

$$\theta_{proj} = 2\theta_{slope} \tag{5}$$

From the point of view of the receiver, it is not important whether the angular scattering of the reflected ray is caused by imperfections of the reflecting surface or a scattering of the light source, supposing that the reflecting surface is ideal: the final effect is the same. Thus, let us consider a light ray coming from a point source S and hitting the surface at point R: if the reflective surface is perfect, the light ray is reflected towards a point Q, whereas, if the surface has some imperfections, which are represented by the rotation θ_{slope}, the ray is deviated by $2\theta_{slope}$ and then reflected towards the point Q'. The same conclusion would, however, be reached if the reflecting surface were perfect, but the incident ray came from an angle of $2\theta_{slope}$ from the original direction, i.e. from a point S'.

This optical property allows us to represent all optical errors as a scattering of the incident rays (i.e., of the light source) and, at the same time, to consider the reflective surface as ideal, greatly simplifying the conceptual model. This scattering is, in turn, further increased by that of the solar source, which cannot be considered as a point source due to the apparent size of the sun and the diffusion of light by the atmosphere. In other words, an effective source distribution $B_{eff}(\theta_{proj})$ of the projected (or reflected) sunrays can be defined which is the result of the convolution of the optical error distribution $E(\theta_{proj} - \theta_{in})$ with the distribution of the light source $B_{source}(\theta_{in})$, as shown by Eq. 6.

$$B_{eff}(\theta_{proj}) = \int_{-\infty}^{+\infty} E(\theta_{proj} - \theta_{in}) B_{source}(\theta_{in}) d\theta_{in} \tag{6}$$

where integration is extended to all incident angles θ_{in} with respect to which the distribution of the source is defined and where $\theta_{proj} - \theta_{in} = 2\theta_{slope}$.

In the model proposed in this work, the $B_{source}(\theta_{in})$ distribution is assumed to be a Gaussian pdf with a standard deviation $\sigma_{source} = 5$ mrad, in accordance with what is proposed by Bendt et al. (1979), where this standard deviation value already accounts for an average daily of the intensity of solar radiation.

However, Richert et al. (2016) suggested a value of 4.1 mrad for σ_{source}, even if they still conservatively used 5 mrad, since this larger value incorporates also specularity errors ($\sigma_{specular} = 0.2$ mrad according to Richert et al. (2016)) and tracking errors ($\sigma_{tracking} = 2$ mrad according to Richert et al. (2016)). In fact, by exploiting the properties of the summation of random variables characterized by Gaussian pdfs, it is possible to write:

$$\sigma_{source} = \sqrt{(\sigma^2_{tracking} + \sigma^2_{specular} + \sigma^2_{sun})} > \sigma_{sun} \tag{7}$$

which justifies the use of a larger value for σ_{source} in the calculations, in particular if $\sigma_{displacement}$ is also present (see Eq. 3).

In this work, the pdf of the optical errors $E(\theta_{proj} - \theta_{in})$, which, based on the model of Bendt et al. (1979), is assumed to be Gaussian with variance equal to that expressed by Eq. 3, will be numerically calculated on the basis of the modeling approach that will be described in next Sections.

2.3. Acceptance angle

The angular acceptance function, represented by $f(\theta)$, is defined as the fraction of incident rays on the collector opening at a certain angle θ from the optical axis. This function is closely related to the geometry and depends on the reflector and receiver configuration. For a parabolic collector, where the aperture angle, or rim angle, is indicated by Φ, having a cylindrical receiver, the acceptance function can be calculated using geometric relationships. From the considerations made in the previous Sections, the angular acceptance function is calculated by considering the collector-receiver system as perfect, free from optical errors, which have already been included in the effective source $B_{eff}(\theta_{proj})$. Denoting by f the focal distance, D the cord and d the diameter of the receiver, we can then define the geometric concentration factor C as:

$$C = \frac{D}{\pi d} \tag{8}$$

The incident rays on the reflective surface at point P, of coordinates (x,y), reach the receiver with an angle of incidence θ (measured from the optical axis) that must satisfy the relation:

$$|\theta| < \theta_x \tag{9}$$

where:

$$\sin\theta_x = \frac{\frac{d}{2}}{2f\left[1+\left(\frac{x}{2f}\right)^2\right]} \tag{10}$$

The limit state, obtained when $|\theta| = \theta_x$, is the one where the rays reach the receiver tangentially. It can be noted how θ_x decreases as the distance of the coordinate x of the point P from the focal axis increases. Then, when $x = D/2$, the angle θ_x assumes its maximum value (called θ_1) for which all incident rays will be accepted. This angle can also be expressed in terms of the rim angle as:

$$\sin(\theta_1) = \frac{\sin(\Phi)}{\pi C} \tag{11}$$

The considerations above imply that the angular acceptance function is equal to 1 for every value $|\theta| < \theta_1$.
Moreover, considering incidence angles θ within the range $(\theta_1 < \theta < \theta_2)$, where the angle θ_2 is such that:

$$\sin(\theta_2) \cong \frac{d}{2f} \tag{12}$$

then, only the central part of the collector opening will be efficient, from $-x_\theta$ to x_θ, where:

$$x_\theta = 2f\left(\frac{d}{2f\sin(\theta)} - 1\right)^{\frac{1}{2}} \tag{13}$$

For angles larger than θ_2 only rays that hit directly the receiver are accepted, but in the present work they are not considered.
Now, for convenience, let us express all the relationships in terms of the rim angle (Φ), considering the existent geometric relation between the different geometric parameters:

$$\frac{D}{4f} = \tan\left(\frac{\Phi}{2}\right) \tag{14}$$

Neglecting any possible complications arising in the cases of low geometric concentration (C), wide incidence angle's (θ) or small aperture angle's (Φ) (cases that are not of interest for the solar energy application), the angular acceptance function for a linear parabolic collector, with cylindrical receiver, can be computed as:

$$f_{PT,cylindrical}(\theta) = \begin{cases} 1 & if\ |\theta| < \theta_1 \\ cot(\theta)\left(\frac{2\,tan\left(\frac{\theta}{2}\right)}{\pi C\theta} - 1\right) & if\ \theta_1 < |\theta| < \theta_2 \\ 0 & if\ |\theta| > \theta_2 \end{cases} \tag{15}$$

2.4. Intercept factor and optical efficiency

Now, by multiplying the angular acceptance function $f_{PT,cylindrical}(\theta)$ by the effective source $B_{eff}(\theta)$, and then integrating over all the incident angles θ, we can obtain the total flux intercepted by the receiver as:

$$q_{in} = \int_{-\infty}^{\infty} d\theta \, f(\theta) B_{eff}(\theta) \tag{16}$$

Dividing now Eq. 16 by the total incident flux, i.e.

$$I_b = \int_{-\infty}^{\infty} d\theta \, B_{eff}(\theta) \tag{17}$$

the intercept factor γ can be finally obtained:

$$\gamma = \int_{-\infty}^{\infty} d\theta f(\theta) B_{eff}(\theta) / I_b \tag{18}$$

which can be simply calculated by any numerical procedure.

This result is exactly equal to that of a detailed ray-tracing analysis, but it is much easier and faster, needing at most three integration steps, which can be performed either analytically, when possible, or numerically.

3. Modeling manufacturing tolerances and assembly/mounting errors

In this Section, the original modifications of the model described above are illustrated with reference to a new design of a common CSP system: the structure of a parabolic trough collector. A full-scale prototype, built in the laboratories of Politecnico di Milano, allowed to prove the feasibility of the new design and to gain experience regarding the assembly steps, as well as the errors that may occur during the construction.

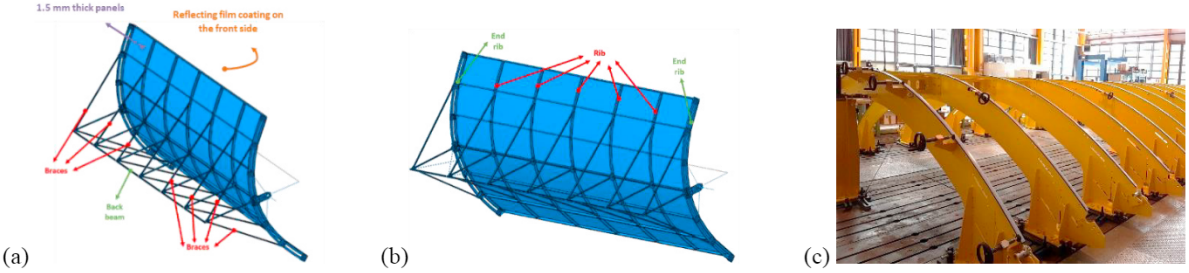

Fig.1. (a) and (b) Back views of the schematization of the parabolic trough; (c) Parabolic jig used for the assembly of the full-scale prototype.

Fig. 1a and Fig.1b schematize the design of the parabolic trough studied in this work. The structure is made by six rows of 1.5 mm thick panels, connected each other by their longer edges. Before the assembly, the two longer edges of the panels are bent in a Z or L shape, so as the Z shape of a panel can be easily connected with the L shape of the adjacent panel. The front side of the structure is coated by a thin film to reflect the sunlight into the receiver tube, placed in the focal point of the parabola. The back side of the structure is reinforced by seven parabolic ribs (Fig.1b) and a V-truss structure made by braces, kingposts and a back beam (Fig.1a).

Fig. 1c shows the parabolic jig used for the assembly of the prototype. It is made by a series of parabolic blades with some supporting tools to fix the position of the parts. The assembly operations start with the placement and connection of the panels, followed by the connection of the ribs and, finally, of the posterior reinforcing structure.

As previously mentioned, the tolerances and errors during production and assembly of the parts of a parabolic trough may directly impact the efficiency of the CSP system. Based on the experience gained during the assembly operations at Politecnico di Milano and the tolerances of the manufactured parts, nine parameters are identified as the most influencing ones on the resulting efficiency of the system. Finally, by means of simple geometrical considerations, every parameter is converted into the resulting angular deviation of the sunlight generated by the involved error.

A short description of the selected nine parameters and their modeling are briefly described hereafter.

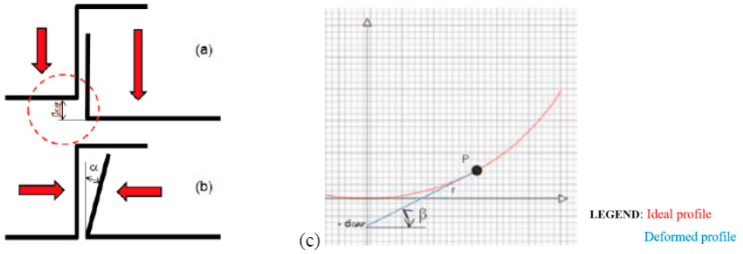

Fig.2. (a) Difference in the relative vertical positioning of two panels adjacent panels d_{gap}; (b) Rotation α of Z or L shape from the perpendicular direction of the panel plane; (c) Error modeling of d_{gap}.

Considering the assembly steps in which adjacent panels are placed on the parabolic jig connected by their Z and L shapes, two main mounting errors might occur. The first involves a difference in the relative vertical positioning of the two panels as shown in Fig. 2a. This parameter was identified as d_{gap} and it might produce a wrongly rotated reflected sunlight from the panel's surface, easily computable by geometrical considerations.

Referring to Fig. 2c, considering the junction at the origin of the axes, it can be assumed that, as a result of the gap created between the two edges, one of the reflecting panels has a different curvature compared to the ideal profile. This curvature can be modeled as a straight line, tangent to the point $P(x_p, y_p)$, where x_p represents the influence length of this error. By imposing the tangency condition between the straight line and the parabola it is possible to find the angular coefficient m of the straight line, given f the focal length of the parabola:

$$y = \frac{1}{4f}x^2 \;\rightarrow\; m = y' = \frac{1}{2f}x \tag{19}$$

determining the equation of the straight line:

$$y_t = \left(\frac{1}{2f}x_P\right)x - d_{gap} \tag{20}$$

Making now the system between the two curve's equations evaluated in point P:

$$\begin{cases} y_P = \frac{1}{4f}x_P^2 \\ y_P = \frac{1}{2f}x_P^2 - d_{gap} \end{cases} \tag{21}$$

it is possible to get the coordinates of point P and the "influence region" x_p of the error:

$$x_P = \sqrt{4f\,d_{gap}} \tag{22}$$

from which it can be computed the slope of the segment $\overline{d_{gap}P}$:

$$\beta = atan\left(\frac{y_P - d_{gap}}{x_P}\right) \tag{23}$$

Therefore, the error in the sunlight reflection produced by d_{gap} is the difference between the ideal slope computed along the parabolic contour in the range $[0, x_p]$, and the angle β previously calculated.

Fig. 2b shows another problem that might occur when the panels are rigidly connected in a wrong way. In the case in which the Z or L shape is rotated by an angle α from the perpendicular direction of the panel plane, the correspondent thin panel rotates producing a deformation, thus affecting the efficiency of the system. The effect of the parameter α was calculated by a FEM numerical simulation, by means of the software Abaqus™, of the positioning of the panel on a parabolic jig, as shown in Fig. 3a.

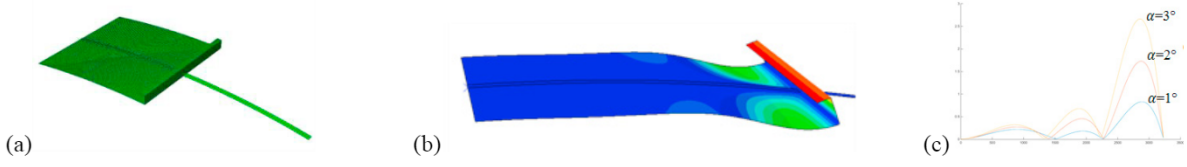

Fig.3. (a) FEM model of the positioning of the panel on a parabolic jig; (b) Graphic view of the results after imposing an angle α; (c) Deformation of the panel imposing different α angles.

The FEM simulations are performed at different folding angles α, obtaining the deformations in the panels shown in Fig. 3b. As can be seen from Fig. 3c, where the x-axis represents the spatial coordinate along the panel's contour and the y-axis refers to the deformations, it is possible to approximate the dependence between the angle α and the resulting deformation by a linear relation. This linearity was also verified from a numerical point of view. The optical errors resulting from deformations, in terms of rotation θ_{proj}^{α}, must multiplied by the factor 2, as shown by Eq. 5. Therefore, the error in the sunlight reflection can be estimated as:

$$\theta_{proj}^{\alpha} = 2 \cdot \mathrm{atan}(y') \tag{24}$$

where y' represents the slope of the function of the deformed shape y of the panel.

For what concern the parabolic jig, both errors on the production and the assembly operations might cause a loss in the efficiency of the system. The errors related to the jig production involve an incorrect surface waviness, that can be identified by two parameters: A_{und} is the amplitude of the deformed jig surface, whereas L_{und} is the half of the wavelength of the profile, as schematized in Fig.4. As discussed later, these two parameters are strictly connected, thus only A_{und} was selected for the sensitivity analysis. It is sufficient to derive the deformed profile to obtain the local rotation, and then multiply it by factor 2 to get the corresponding sunlight reflection error θ_{proj}^{jig}.

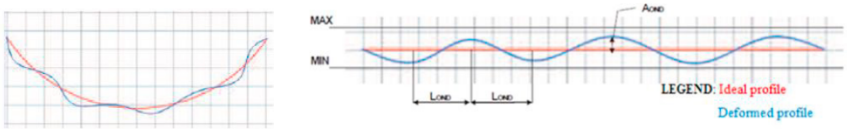

Fig.4. Schematization of the jig's deformed shape caused from the waviness identified by A_{und} and L_{und}.

The errors related with the jig positioning involve the horizontal and the vertical offsets from the ideal position, and the wrong rotation, respectively identified by $\Delta x_{off,jig}$, $\Delta y_{off,jig}$ and $\Delta\theta_{collector}$. Considering the horizontal offset, referring to the scheme in Fig.5a, it is possible to state that the error, represented by the angle φ, corresponds to the sunlight reflection error due to the horizontal displacement of the parabola (it does not require to be multiply by the factor 2). Relying on a simply trigonometric approach, the error can be directly computed as:

$$\varphi = \epsilon - \theta \tag{25}$$

where the angles θ and ϵ can be obtained by geometrical considerations:

$$\theta = \mathrm{atan}\left(\frac{x}{f-y}\right) \tag{26}$$

$$\epsilon = \mathrm{atan}\left(\frac{x+\Delta x_{off,jig}}{f-y}\right) \tag{27}$$

where $\Delta x_{off,jig}$ represents the horizontal offset and x and y represent the correct horizontal and vertical parabolic coordinates. The same procedure can be applied to compute the errors in the cases of the vertical offset and the rotation. The only differences are in the needed parameters ($\Delta y_{off,jig}$ and $\Delta\theta_{collector}$) and in the geometric references (Fig.5b and Fig.5c). It worth to mention that the position and rotations of the jig in the third direction were not considered since they had a much lower influence on the intercept factor.

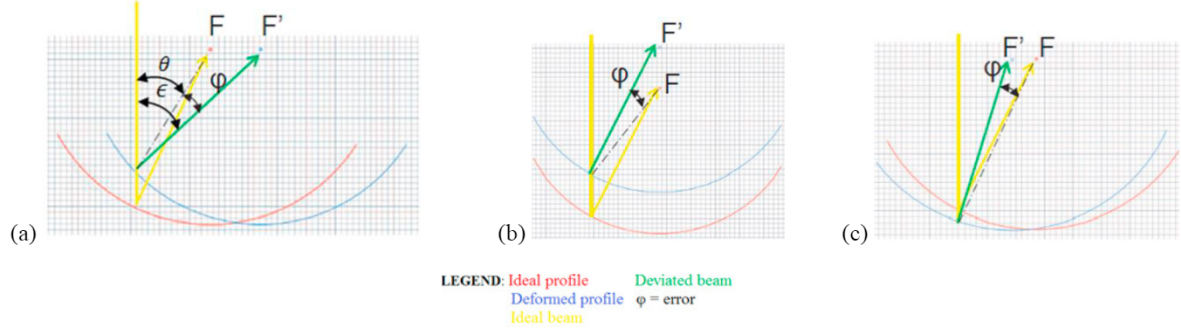

Fig.5. Schematization of: (a) Horizontal offset of the jig $\Delta x_{off,jig}$; (b) Vertical offset of the jig $\Delta y_{off,jig}$; (c) Rotation of the jig $\Delta\theta_{collector}$.

Finally, also the positioning of the receiver relative to the ideal position of the jig might be very influent. Therefore, the horizontal and the vertical offsets of this element were considered for the sensitivity analysis, respectively identified by $\Delta x_{off,rec}$ and $\Delta y_{off,rec}$ and shown in Fig.6a and Fig.6b. The correspondent errors can be treated again by trigonometry modeling, exactly in the same way as done for the offsets of the jig. The error φ, again, does not need the multiplication factor 2, since it already represents the reflected sunlight error.

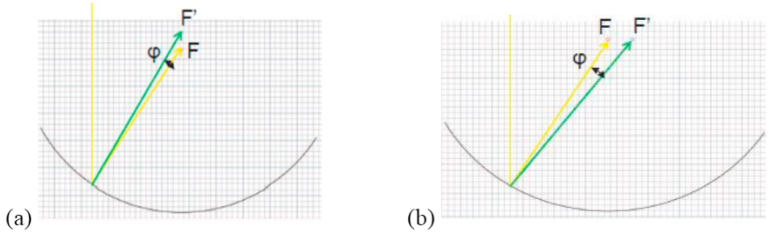

Fig.6. Schematization of: (a) Horizontal offset of the receiver $\Delta x_{off,rec}$; (b) Vertical offset of the receiver $\Delta y_{off,rec}$.

It is worth to mention that many other parameters might affect the intercept factor, but their contribution was estimated to be negligible for a preliminary efficiency analysis.

4. Sensitivity analysis methodological approaches

As shown in the previous Sections, the overall optical efficiency of a CSP system is a function of the parabolic trough intercept factor, which, in turn, depends on several parameters. These parameters are then the inputs of the proposed semi-analytical model, whose output is the intercept factor. As already illustrated in the Introduction, the input parameters, i.e., in our case, the manufacturing tolerances and the assembly/mounting errors, are uncertain by nature, which means that they are not precisely known and that they are in general different for each parabolic trough of a solar field. These uncertainties, represented, as we have seen, by suitable pdfs, "propagate" through the model and affect the output, so that the intercept factor (and consequently the optical efficiency) becomes uncertain itself. In this framework, it becomes clear how important is the task of assessing the impact of each input uncertainty on the variability of the output. In the present study this task entails identifying the manufacturing tolerances and the assembly/mounting errors whose uncertainties most influence the variability of the intercept factor. This kind of information is, in fact, of utmost importance for the system designer/operators, because it would allow to effectively target improvements of the design aimed at achieving the best compromises between the solar field production and its costs.

This kind of analysis in generally known as sensitivity analysis (SA). Several methods are available in literature for performing sensitivity analysis. Usually they are divided in two major types of approaches, local and global methods. Local approaches (Local Sensitivity Analysis - LSA) focus on the local impact that input parameters have on the final output by evaluating the effects of small input variations, taken one at a time. Global approaches (Global Sensitivity Analysis - GSA), on the other hand, consider the effects that simultaneous variations of the input parameters have on the model output, accounting for the entire range of variability of the inputs. In this work we follow a typical strategy adopted in literature works on sensitivity analysis, i.e., we start applying a simple, intuitive local method, which provides a first quick glance on the input/output relationship, and then we proceed by performing a more complete, and indeed more computationally intensive, global sensitivity analysis. Usually, the first LSA stage is used to perform a first screening out of the most important input parameters and then a GSA is carried out on the restricted set of input parameters selected in the first SA stage. In fact, GSA performed over larger dimensional input spaces would quickly become unfeasible from a computational point of view [Granger Morgan and Henrion (1990)]. Here, benefiting from the fact that the proposed semi-analytical model is very fast and not computationally too demanding, we will be able to perform both LSA and GSA on the same set of input parameters.

Thus, we propose here to start the SA by applying a local approach often referred to in literature as "nominal range sensitivity analysis (NRSA)", as, for example, reported by Granger Morgan and Henrion (1990). It is possible to say that, actually, this method is more than a local approach, since it somehow accounts for the whole range of variability of the input parameters (although only extreme values of the range are considered), but, at the same time it is not a global method, since the inputs are varied one at a time (keeping the others constant), so that the interactions among are not taken into account. In general, given a model m describing the relationship between n input parameters x_i, $i = 1 \dots n$, and an output y, it is possible to measure the effect of the variability of a single input x_i on the variability of the output y by defining of the following indicator:

$$U_R(x_i, y) = m\left(x_i^+, x_{j\neq i}^0\right) - m\left(x_i^-, x_{j\neq i}^0\right) \tag{28}$$

where x_i^+ and x_i^- are the maximum and the minimum values, respectively, of the variability input x_i range, whereas the quantities $x_{i\neq j}^0$ are the nominal values of all the other inputs $x_{j\neq i}$. The SA carried on using this approach benefits from the advantage of being very intuitive and fast, needing a small number of model evaluations m. However, the evaluation of the output y at the extremes of an individual input variability range, keeping all the other at the nominal values, does not allow to estimate the effect of the combinations of the different errors, as previously mentioned.

In this work, the model m is that proposed in the previous Section for the calculation of the intercept factor. The inputs x_i, shown in Tab. 1, are the selected model's parameters, associated to the tolerances and to the assembly/mounting errors previously described, whereas the output is the intercept factor γ.

Table 1. Considered variability ranges for the chosen parameters.

Symbol	Range of values	Unit of measure
d_{gap}	[0, 4]	[mm]
α	[0, 3]	[°]
A_{und}	[0, 2]	[mm]
$\Delta x_{off,jig}$	[0, 1]	[mm]
$\Delta y_{off,jig}$	[0, 1]	[mm]
$\Delta x_{off,rec}$	[0, 15]	[mm]
$\Delta y_{off,rec}$	[0, 15]	[mm]
$\Delta\theta_{collector}$	[0, 1]	[°]

Tab. 1 also shows the variability ranges of each input, chosen on the basis of engineering considerations and on the experience acquired on the CSP prototype built at the Politecnico di Milano. Note that the lower values of each variability range correspond to having no tolerances/errors. These values are assumed as the nominal ones, i.e., $x_i^0 = x_i^-$ for the NRSA. Therefore, the NRSA implies the computation of the intercept factor at the minimum (no error $\rightarrow \gamma = 1$) and maximum value for each tolerance/error, considered one at a time time and fixing all the other inputs to their nominal values (i.e., the lowest value of the range). Thus, the indicator $U_R(x_i, y)$ defined by Eq. 28 turns out to correspond to the loss of intercept factor due to any individual error/tolerance.

Note that this kind of analysis is such that there is no need for computing the indicator U_R for the special parameter L_{und}, since, imposing $A_{und} = 0$ (i.e., its nominal value), implies that L_{und} has no effects on the intercept factor, as clearly shown in Section 3. In other words, the parameters L_{und} and A_{und} are not fully independent. However, the NRSA is not capable of coping with this kind of effects, and the consequence is that we cannot estimate the sensitivity index for L_{und}. This problem will be overcome by the application of a GSA method later in this Section. Here the analysis is performed by setting the wavelength of the jig undulation as fixed to 300 mm, a value identified on the basis of engineering experience.

Furthermore, in order for the analysis to be more realistic, we resort to probabilistic modeling of the error/tolerances d_{gap}, α and A_{und}, for accounting for the fact that these parameters characterize the geometry of the parabolic trough at different locations (as already described in Section 3), where in general, they take different values.

The variation of the parameter A_{und} along the parabolic profile and its modeling as a random variable has already been discussed in Section 3. With regards to the parameter d_{gap}, different values are considered for each coupling between two panels on the xy plane, and for the two edges at the extremes of the trough, for a total number of locations equal to 12. Operatively, for the calculation of the intercept factor, the values of d_{gap} are sampled from a uniform distribution $U(d_{gap})$ defined over the variability range of d_{gap}. Similar considerations can be made also for the parameter α, whose 12 values for a single trough are operatively sampled from a uniform distribution $U(\alpha)$ defined over its range of variability. The choice of uniform pdfs for representing the randomness of these parameters is motivated by the fact that, without any precise additional knowledge of the manufacturing and assembly processes, these distributions are more suitable to describe the parameter variability along the trough profile. This choice also allows to automatically discard values of the parameters which are larger than the target prescriptions and quality control requirements.

In order to assess the effect that the entire range of variability has on the intercept factor, in the calculation of the intercept factor (i.e., the output of the proposed model), we run the model 1000 times in correspondence of different realizations of the parameters d_{gap}, α and A_{und} (thus obtaining different values of the intercept factor) and then we average all the outputs obtained out, so that we obtain an average intercept factor which depends only on the amplitude of the input variability ranges (related to the manufacturing and assembly/mounting processes), and not on the spatial variations.

The results of the analysis, in terms of average percentage of optical efficiency loss with respect to the ideal conditions (that is the configuration with no errors and intercept factor $\gamma = 1$), are reported in Tab. 2. The LSA is performed in correspondence of different possible variability ranges, to highlight also the effects that different manufacturing and assembly/mounting processes can have on the optical efficiency uncertainty (or variability): better, and more expensive, processes in general should lead to narrower ranges of variability of the input parameters.

The most important parameters turn out to be d_{gap}, α, A_{und}, $\Delta x_{off,rec}$ and $\Delta\theta_{collector}$, whereas the optical efficiency losses due to the other parameters is almost negligible and are thus not reported in Tab. 2. Among these five errors/tolerances, the

$\Delta\theta_{collector}$ parameter seems the most important when the broader input variability ranges are considered, since a tolerance of ±1° implies a 16.7% loss on the optical efficiency. In other words, the uncertainty range of the parameter $\Delta\theta_{collector}$ is such that the intercept factor may vary from 1 to approximately 0.83, with a significant reduction of the optical performances. However, when the variability ranges are reduced, the importance of the parameter $\Delta\theta_{collector}$ decreases very fast, along with those of the parameters α and A_{und}, so that the parameter d_{gap} becomes the most important in the deterioration of the optical efficiency, when better manufacturing/assembly/mounting processes are adopted.

Table 2. Sensitivity analysis' results on nominal range for different variability ranges of errors/tolerances.

$\boldsymbol{d_{gap}}$ [mm]	**0 - 4**	**0 – 3**	**0 - 2**	**0 - 1**
Δy [%]	-8,40%	-6,82%	-4,98%	-2,75%
$\boldsymbol{\alpha}$ [°]	**0 - 3**	**0 – 2**	**0 - 1**	**0 - 0,5**
Δy [%]	-14,70%	-8,48%	-2,32%	-0,40%
$\boldsymbol{A_{und}}$ [mm]	**0 - 2**	**0 – 1**	**0 - 0,5**	**0 - 0,1**
Δy [%]	-10,08%	-2,02%	-0,38%	-0,05%
$\boldsymbol{\Delta x_{off,rec}}$ [mm]	**0 - 15**	**0 – 10**	**0 - 5**	**0 - 2,5**
Δy [%]	-2,12%	-0,74%	-0,21%	-0,09%
$\boldsymbol{\Delta\theta_{collector}}$ [°]	**0 - 1**	**0 - 0,5**	**0 - 0,25**	**0 - 0,05**
Δy [%]	-16,65%	-2,08%	-0,38%	-0,08%

The results contained in Tab. 2 are also graphically represented in Fig. 7, where also the other less influent parameters' trends are shown. As expected, decreasing the widths of the nominal variability ranges (the labels in the *x* axis indicate the column of results in Tab. 2 moving from left to right), the optical efficiency losses (or variations) also decrease.

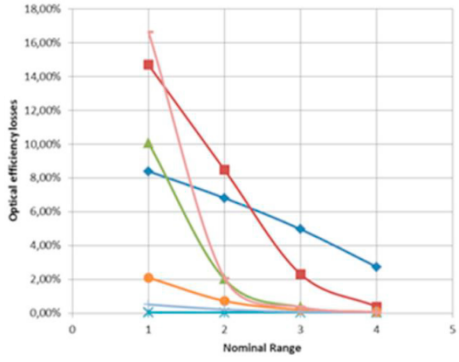

Fig.7. Graphical trend of the SA on nominal range results. Pink line: $\Delta\theta_{collector}$; red line: α; green line: A_{und}; dark blue line: d_{gap}; orange line: $\Delta x_{off,rec}$; violet line: $\Delta y_{off,rec}$; light blue line: $\Delta x_{off,jig}$ and $\Delta y_{off,jig}$.

As anticipated above, these results are very helpful to the designer, however, they must be taken with care, since LSA techniques only provide a rough idea of the underlying relationships between the input and the output variabilities in a given model. Indeed, GSA methods more effectively capture the dependence of the model output variability on the variability of the input parameters, by accounting for the entire range of variability of the inputs and for their possible synergies (or "interactions") as shown in Granger Morgan and Henrion (1990), among many other literature works. The major drawback of these techniques, which often severely limits their application, is that they typically require unaffordable computational efforts, requiring a very large number of model evaluations. This issue becomes even worse when dealing with complex the models, taking long computational times to provide a single output evaluation. On the other hand, the model that we propose in this work for the computation of the intercept factor allows to partially overcome this issue, since its semi-analytical nature guarantees fast calculations, as opposed, for example, to the commonly used ray-tracing approaches.

Thus, in this work we attempt to perform a GSA by resorting to an analysis of variance (ANOVA) method. The viewpoint of these methods is such that, given a generic model $y = m(\boldsymbol{\theta_\varphi})$, each input parameter ($\boldsymbol{\theta_\varphi}$) variability, represented in terms of proper pdfs, contributes to the total unconditional variance of the output $\sigma^2(y)$. With regards to this point, it can be shown that the unconditional variance of the model output y can be decomposed as:

$$\sigma^2(y) = \sigma^2\left(E\left[y|\theta_{\varphi i}\right]\right) + E\left[\sigma^2(y|\theta_{\varphi i})\right], \quad i = 1,\dots,k \tag{29}$$

where k is the number of uncertain inputs and $\theta_{\varphi i}$ is one of the input parameters collected in the vector $\boldsymbol{\theta_{\varphi}}$. Note that, in our application, the output y is the intercept factor γ, whereas the parameters $\theta_{\varphi i}$ are the manufacturing tolerances and assembly/mounting errors. Therefore, the conditional variance $\sigma^2\left(E\left[y|\theta_{\varphi i}\right]\right)$ represents the contribution to the total variance only due to the parameter $\theta_{\varphi i}$ alone, whereas the term $E\left[\sigma^2(y|\theta_{\varphi i})\right]$ collects the contributions relate to the variability of all other parameters. The first term is often called *main effect*: it is used as an indicator of the importance of $\theta_{\varphi i}$ contributing to the variance of y, i.e. the sensitivity of y with respect to $\theta_{\varphi i}$. By normalizing the main effect of $\theta_{\varphi i}$ by the unconditional variance of the output, we obtain the first order sensitivity index:

$$Si_i = \frac{\sigma^2(E[y|\theta_{\varphi i}])}{\sigma^2(y)} \tag{30}$$

However, the first order sensitivity indexes do not take into account the interactions between input factors. Two factors are said to interact if their total effect on the output is not the sum of their first order effects. The effect of the interaction between two factors $\theta_{\varphi i}$ and $\theta_{\varphi j}$, for $i \neq j$, on the final output y can be found as:

$${\sigma_{ij}}^2 = \sigma^2\left(E\left[y|\theta_{\varphi i}, \theta_{\varphi j}\right]\right) - \sigma^2\left(E\left[y|\theta_{\varphi i}\right]\right) - \sigma^2\left(E\left[y|\theta_{\varphi j}\right]\right) \tag{31}$$

where $\sigma^2\left(E\left[y|\theta_{\varphi i}, \theta_{\varphi j}\right]\right)$ describes the joint effect of the pair $(\theta_{\varphi i}, \theta_{\varphi j})$ on y. This effect is known as the second-order effect. It is important to highlight that in a model without interactions, the first order indexes sum up to one. Homma and Saltelli (1996) proposed an extension for direct estimation of the overall effect of $\theta_{\varphi i}$ on the output y, by summing the main effect of $\theta_{\varphi i}$ and all its interactions with other parameters. By normalizing this estimation with the unconditional variance, the estimation of the so-called total sensitivity index, indicated by Si_i, can be obtained. Again, the uncertainties associated to each input variable is assumed to be described by uniform pdfs. Tab. 3 shows, for each parameter, the mean and the half width of each uniform pdf used. It can be noted that for all the parameters, except for d_{gap} and A_{und}, the mean value is equal to zero and the corresponding variability range is symmetric (negative and positive interval are equal), whereas for the two parameters d_{gap} and A_{und} the mean value is different from zero and the considered range is only positive. These parameters are, in fact, measured in relative terms with respect to the ideal profile.

Many Monte Carlo, sampling-based numerical techniques have been proposed in literature for estimating the Sobol indices of a GSA: here we adopted a scheme proposed by Homma and Saltelli (1996) which allows to achieve good efficiencies (i.e., lower number of intercept factor evaluations).

Table 3. Input values for the GSA model.

Symbol	Mean value	Half width [±]
d_{gap}	2 mm	2 mm
α	0°	3°
A_{und}	1 mm	1 mm
L_{und}	300 mm	0 mm
$\Delta x_{off,jig}$	0 mm	1 mm
$\Delta y_{off,jig}$	0 mm	1 mm
$\Delta x_{off,rec}$	0 mm	15 mm
$\Delta y_{off,rec}$	0 mm	15 mm
$\Delta\theta_{collector}$	0°	1°

The plots of Fig. 8 show the satisfactory convergence (over 10^5 model evaluations) of the main (8a) and the total (8b) Sobol sensitivity indexes achieved during the GSA: the plots are limited to the first 10^4 model evaluations for the sake of readability, with no loss of information. Tab. 4 and Tab. 5 report the ranking of the main and the total sensitivity indexes obtained for the input parameters, limited to the first five positions. Note that the parameter L_{und}, whose variability turns out anyway not too be very important, does not pose any problems to the Sobol-based GSA (as opposed to LSA, see above), since the dependencies among the input variables are automatically taken into account. Interestingly, the more complete SA based on the estimation of the Sobol indexes confirms the results obtained with the much leaner LSA.

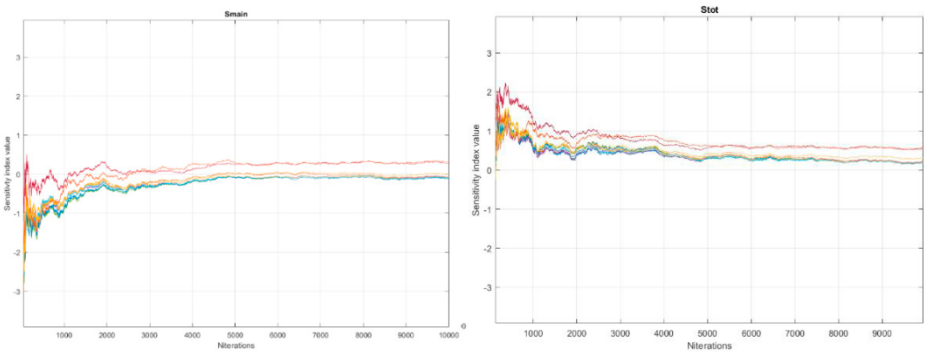

Fig. 8. (a) Main sensitivity indexes for increasing number of intercept factor evaluations; (b) Total sensitivity indexes for increasing number of intercept factor evaluations. Different colors refer to the various input parameters.

Table 4. Ranking of the main Sobol sensitivity indexes.

Position	1st	2nd	3rd	4th	5th
Parameter	$\Delta\theta_{collector}$	$\Delta x_{off,rec}$	α	A_{und}	d_{gap}

Table 5. Ranking of the total Sobol sensitivity indexes.

Position	1st	2nd	3rd	4th	5th
Parameter	$\Delta\theta_{collector}$	$\Delta x_{off,rec}$	α	A_{und}	d_{gap}

5. Conclusions

The work presented in this paper has regarded the optimization of the performances of parabolic solar collectors and, more generally, of large-scale structures. A methodological approach for the design of modern parabolic collectors has been originally extended to be able to directly account for manufacturing tolerances and assembly/mounting errors. The semi-analytical nature of the model, which has been preserved by our modifications, is of great importance because, on one side, it allows to track the functional relationships between the design parameter and the optical efficiency, and, on the other side, because it guarantees fast calculations of the intercept factor require rather low computational expenses.

Thus, the proposed model is a valuable tool for a designer who aims at optimizing the manufacturing and assembly/mounting processes of a parabolic trough-based CSP system for improving its efficiency and maximizing the economics of the plant. In order to demonstrate these capabilities, in this work we have used the model for performing both a simple local (based on the nominal range sensitivity analysis method) and a more demanding global (based on the ANOVA and the estimation of the Sobol indexes) sensitivity analysis aimed at quantifying the impact of the model input uncertainties on the intercept factor.

From an engineering point of view, the results of the sensitivity analyses highlighted the importance of focusing on the tolerances/errors d_{gap}, α, A_{und}, $\Delta x_{off,rec}$ and $\Delta\theta_{collector}$ only, if the main design goal is that of achieving the highest possible intercept factor. Albeit all the parameters were somehow expected to have a significant impact on the optical performances of the CSP, on the basis of the engineering common sense, the parameter $\Delta\theta_{collector}$ has unexpectedly resulted to have the largest influence on the intercept factor, so that special care should be given by a designer in accurately limit and control this error.

Due to the speed of the semi-analytical framework proposed, the SA analyses required affordable computational times. In fact, while the local nominal range SA required just few minutes for each parameter considered (approximately 10-15 minutes), the global ANOVA-based SA has not exceeded one day of calculations. Both analyses have been performed using the software MATLAB, version R2017b, running on an IntelCore i3 CPU 540 at 3.07 GHz, based on a 64-bit operating system and with 8 GB RAM.

These promising results foster future works aimed at coupling the model for the intercept factor calculation with a cost model in order to be able to devise proper optimization strategies.

References

Bendt, P., Rabl, A., Gaul, H.W., Reed, K.A. (1979). *Optical analysis and optimization of line focus solar collectors*. NASA STI/Recon Technical Report N. 11.

Dinter, F., Gonzalez, D. M. (2013). *Operability, reliability and economic benefits of CSP with thermal energy storage: First year of operation of ANDASOL 3*, Energy Procedia 49, 2472–2481.

Fend, T., Qoaider, L. (2011). *Chapter 1: Introduction* in enerMENA CSP Teaching Materials, German Aerospace Center (DLR), Cologne, pp. 1–6.

Granger Morgan, M., Henrion, M.. (1990). Uncertainty: A Guide to Dealing with Uncertainty in Quantitative Risk and Policy Analysis, Cambridge: Cambridge University Press.

Homma, T., Saltelli, A. (1996). *Importance measures in global sensitivity analysis of nonlinear models*, Reliability Engineering & System Safety 52, Issue 1, 1-17.

IRENA (2015). *Renewable power generation costs in 2014*.
Mehos, M., Turchi, C., Jorgenson, J. (2016). *On the Path to Sunshot: Advancing Concentrating Solar Power Technology, Performance, and Dispatchability*. NREL. Golden, CO.
Richert, T., Riffelmann, K.J., Nava, P. (2016). Mitigating project risk by use of high performance collector technology. AIP Conference Proceedings 1734.
U.S. Department of Energy, Office of Efficiency & Renewable energy (2017). *Energy.gov, SunShot initiative*. Online, accessed in February 2017, available at: https://energy.gov/eere/sunshot/sunshot-initiative.